Global Environmental Change 71 (2021) 102370

Contents lists available at ScienceDirect

Global Environmental Change

journal homepage: www.elsevier.com/locate/gloenvcha

Do we prioritize floodplains for development and farming? Mapping global dependence and exposure to inundation

Rachel Dryden [a,b,*], Mira Anand [a], Bernhard Lehner [a,*], Etienne Fluet-Chouinard [c,1]

[a] *Department of Geography, McGill University, 805 Sherbrooke Street West, Montréal H3A 0B9, Québec, Canada*
[b] *RAND Corporation, 4570 Fifth Ave #600, Pittsburgh, PA 15213, USA*
[c] *Center for Limnology, University of Wisconsin-Madison, 680 North Park Street, Madison, WI 53706, USA*

ARTICLE INFO

Keywords:
Floodplain
Inundation
Dependence
Exposure
Population
Agriculture

ABSTRACT

Global wetlands and floodplains offer benefits and perils alike for human society. For example, humans rely on natural flood cycles for fisheries and agriculture, yet flooding also caused nearly one trillion USD in damage in the past 30 years and impacts millions of people every year. Looking forward, altered flow regimes or increased drought conditions are expected to affect the natural inundation cycle and its ecosystem services. The current and potential future impacts of flooding and drying events warrant increasing efforts to quantify our dependence and exposure within flooded areas, since any change from current inundation patterns is expected to have consequences for those who rely on regular flood occurrences. This paper provides a baseline global assessment of the dependence and exposure of human populations, urban areas, roads, and agriculture on current inundation patterns. The analysis uses a spatially explicit inundation map at ~500 m resolution (GIEMS-D15) derived from satellite remote sensing to represent flooding extents and overlays it with current population and land use maps. We find that 35% of the analyzed population, or 2.0 billion people, live inside areas that are prone to inland flooding, which comprise only 12% of the land surface area (excluding marine coastal areas), confirming that population densities within inundation zones are about three-times above global average. Likewise, 35% of urban areas potentially experience regular, seasonal, or infrequent flooding. Agriculture shows a similar pattern with 24% of the world's cropland in areas of recurring inundation. Finally, we estimate that 18% of the global road network is exposed to inundation during high water periods. These global estimates demonstrate a preferential tendency of human populations, infrastructure, and agriculture to be co-located within inundation areas, making related anthropogenic activities highly susceptible to future changes in flood regimes. The results are intended to offer a suite of first-order estimates as partial input to more holistic risk and vulnerability assessments and to ultimately improve environmental planning and policy at large scales.

1. Introduction

Wetlands and floodplains, typically low-lying areas that experience seasonal or intermittent inundation, are hotspots of biological productivity (Zhong et al., 2015) and ecosystem service provision (Verhoeven and Setter, 2010; Costanza et al., 2014) yet only occupy 2–10% of total global land area depending on how they are defined (Nakaegawa, 2012). Hydrologically active riverine floodplains are key regulators of vital environmental processes, including groundwater recharge and evapotranspiration. Hydrologically active riverine floodplains depend on a flood pulse (Junk et al., 1989) of river discharge, characterized by the timing and magnitude of its high flows, which is largely driven by rainfall or snow-melt in the upstream drainage area. Historically, human populations have settled along rivers to gain direct access to freshwater resources for consumption and sanitation, to produce and harvest food and timber from their floodplains, to utilize riverine services such as fisheries, transportation and wastewater disposal, or simply to enjoy their aesthetic, recreational, or spiritual value (Mays, 2010; Kummu et al., 2011; Hanna et al. 2018). As a result, today's floodplains are deemed critical for a large variety of benefits and services (Tockner and Stanford, 2002; Falkenmark et al., 2007), including agriculture (Gonçalves et al., 2010) and the construction of settlements and roads due to

* Corresponding authors at: RAND Corporation, 4570 Fifth Ave #600, Pittsburgh, PA 15213, USA (R. Dryden), Department of Geography, McGill University, 805 Sherbrooke Street West, Montréal H3A 0B9, Québec, Canada (B. Lehner).
E-mail addresses: rsterato@rand.org (R. Dryden), bernhard.lehner@mcgill.ca (B. Lehner).
[1] Present address: Department of Earth System Science, Stanford University, Stanford, CA 94305, USA

https://doi.org/10.1016/j.gloenvcha.2021.102370
Received 19 April 2020; Received in revised form 1 September 2021; Accepted 4 September 2021
Available online 19 October 2021

the inherent convenience of building on flat terrain (Acreman et al., 2003). Despite the recognized importance of floodplains in human society, quantified assessments of the extent of human floodplain use and dependence are limited.

1.1. Human populations

Throughout history, humans have settled near fertile lowlands and alluvial plains because of their important role in food supply—through floodplain fisheries and subsistence farming—as well as other direct (e.g., water supply, recreation) and indirect (e.g., cultural or religious) ecosystem services (MEA, 2005). Although historically people may have prioritized lowlands that only flooded rarely, technical advancements in drainage, waterworks, and protective infrastructure (such as levees and dams), allowed anthropogenic land use to encroach into flood-prone areas. Today, about half of the world's population lives within 3 km of a surface freshwater body (Kummu et al., 2011), and similarly, more than half of the global population has settled within 200 km of the coast (Ding, 2015). This proximity to waterways makes our society dependent on the benefits of seasonal or regular flooding but also vulnerable to infrequent extreme events. Shifting flood regimes can manifest as increased or decreased inundation or changes in the timing of flooding and drying, which may have positive or negative consequences depending on the socio-environmental context. In regions that are prone to more extreme floods or droughts, unpredictable streamflow exposes human populations and their activities to potentially catastrophic riverine inundation or severe surface or soil water shortages that put water and food production at risk.

Global records show between 20 and 300 million people are affected by flooding each year, yet these numbers vary widely and may be underreported (Hirabayashi and Kanae, 2009). Results from studies with different definitions and methods have exceeded these values: for example, Dilley (2005) reports that one-third of global land area is flood-prone and 82% of the global population are affected by flooding. In the last three decades, recorded inland floods (i.e., from riverine sources) claimed more than 0.66 million lives, displaced more than 636 million people, and exceeded 800 billion USD in economic damage on a global scale (summed results from the Dartmouth Flood Observatory Global Active Archive of Large Flood Events, http://floodobservatory.colorado.edu/Archives). The EM-DAT disaster database, (https://www.emdat.be), cross-referenced by the International Water Management Institute (IWMI), reports 0.21 million deaths worldwide between 1980 and 2011, and 3 billion people affected (including deaths, injuries, and people made homeless).

1.2. Urbanization and road infrastructure

Floodplains provide easy urban development on flat terrain, transport and trade along waterways, access to water supply (either river water or groundwater in alluvial floodplain aquifers that are replenished during inundation events), and wastewater disposal. However, urban areas, and the road networks that connect them, face unique challenges related to inundation. Urban floods typically impact more populous communities (Wheater and Evans, 2009) since more than 50% of the global population now lives in urban areas (United Nations, 2010). Rising costs of fixed infrastructure (Ding, 2015) and disruption of road networks that provide access to resources, employment, and other human activities (Amador-Jimenez and Willis, 2012) are increasing the economic exposure to flooding. Several examples at the local scale show increased settlements in hazard-prone areas of Africa (Douglas et al., 2008). In Asia, floodplain development is most intensive in populous catchments, i.e. in areas with population densities of more than 200 people per km^2; and 60–99% of Asian riparian corridors have either been urbanized or converted to cropland (Tockner and Stanford, 2002).

A recent shift towards nature-based solutions includes approaches such as Blue-Green cities (Lawson et al., 2014) and China's 'sponge cities' (Chan et al., 2018). Rather than controlling or diverting floods, these methods restore natural hydrological functioning to increase resilience by utilizing wetlands, natural waterbodies, and green infrastructure that support infiltration and ephemeral surface water. This approach mitigates disastrous flooding and dry periods and also provides urban populations with ecosystem service benefits of regular inundation, such as improved water quality, higher biodiversity, and socio-cultural services (Lawson et al., 2014).

1.3. Agriculture

Nearly 25% of the total global land area was converted for cultivation by the year 2000, with cropland comprising more than 50% of land area in several river basins in India, including intensive cultivation of the flood-prone Ganges and Brahmaputra basins (Subbiah et al., 2001), and more than 30% in other parts of Asia (MEA, 2005). In Africa, an estimated 3 million people depend on floodplains for agriculture (Richter et al., 2010), and several hundred thousand households rely on fisheries (Junk et al., 2013). Populations that practice flood recession agriculture benefit from seasonal flooding and depend on its predictability, as loss of inundation or excess water could jeopardize the food supply and vegetation necessary for animal grazing in the dry season (Richter et al., 2010). Likewise, rice paddies rely on specific amounts of inundation, and rice productivity has been shown to both increase and decrease with the strength of the summer monsoon, depending on regional variation and time of year (Asada and Matsumoto, 2009), with extreme floods leading to severe crop loss (Fox and Ledgerwood, 1999). Non-irrigated agriculture in floodplains where seasonal inundation replenishes soil moisture may be threatened by droughts or extended low flow periods, often caused by reduced discharge from distant upland regions.

1.4. Study objectives

Human populations globally rely on floodplains for ecosystem service provision, while also facing exposure to potentially adverse impacts, such as loss of life (Jonkman, 2005) and economic damage (Merz et al., 2010). The projected effects of climate and land-use changes on inundation patterns are expected to put additional stress on these interdependencies. Reliable estimates of the global presence of humans and their assets in floodplains are thus urgently needed. Typically, the focus of past studies has been on the 'exposure' side of the issue, i.e. "*the presence of people, livelihoods, species or ecosystems, environmental functions, services and resources, infrastructure, or economic, social, or cultural assets in places and settings that could be adversely affected*" (IPCC, 2014). However, inundation can also have beneficial effects on humans and ecosystems, such as through increased biodiversity and fishery production, flood recession agriculture, groundwater recharge, and coastal mangroves. Thus, our study expands its scope to include not only exposure but also overall human 'dependencies' on current inundation patterns (*sensu* exposure with 'positive' rather than 'adverse' effects). We acknowledge that positive floodplain dependencies also exist for people who live beyond the physical boundaries of inundated areas, such as through interlinked economies or trade; however, in this study, we limit our assessment to people, agriculture, and development located within inundated areas for lack of information on these teleconnections at a global scale.

Various flood-risk assessments have been undertaken in the past to quantify the exposure of humans and their assets, most commonly at the local, regional, or national scale (e.g., Douglas et al., 2008; Pradhan, 2009; Lugeri et al., 2010). A number of global studies also estimated flood exposure of populations (Jongman et al., 2012; Hirabayashi et al., 2013; Ward et al., 2013; Winsemius et al., 2013, 2016; Tellman et al., 2021), with a focus on projecting the effects of specific changes in flood frequencies as a result of climate change to understand potential future impacts. However, these studies are often limited by spatially coarse input data and their respective estimation uncertainties. In particular, recent evaluations using higher-resolution flooding and population data showed that previous flood risk analyses performed on coarser-resolution population data may have overestimated the number of people exposed to flooding (Smith et al., 2019). Other risk studies also exist, but they have either included flooding as only one of many hazards (e.g., Peduzzi et al., 2009), have considered exposed populations as only one of many contributing factors of overall flood vulnerability (e.g., Balica et al., 2009), or were limited in geographic scope (e.g., Balk et al., 2012).

Agriculture in areas experiencing inundation is an even more understudied topic at the global scale. Previous assessments have estimated agricultural vulnerability, particularly in terms of economic damage (Merz et al., 2010) or in reference to arable lands exposed to drought hazards (Peduzzi et al., 2009). Case studies and estimates of the impacts of flooding on agriculture exist for several important agrarian regions (Hall et al., 2005; Ngoc Chau et al., 2013; Foudi et al. 2015; Zhang et al., 2015). Yet, comprehensive global scale assessments of agricultural floodplain dependence, in addition to exposure, are lacking.

In this study, we explicitly assess the spatial extent of human occupation and activity within areas prone to regular inundation on a global scale. Unlike previous global studies, we assume that a high density of humans and their assets in periodically flooded areas represents a strong dependence on, or exposure to, both the benefits and perils of inundation. As a proxy for this dependence and exposure, we quantify the spatial overlap of inundation areas with populations, urban areas, roads, and agriculture at a global scale, including areas of both regular and seasonal (i.e., potentially beneficial) and infrequent (i.e., potentially damaging) inundation.

Our analyses are based on mapped inundation surfaces of varying extents (GIEMS-D15; Fluet-Chouinard et al., 2015). GIEMS-D15 captures both intra- and inter-annual flooding at ~500 m spatial resolution. Importantly, GIEMS-D15 represents natural and artificial inundated surfaces, including rice paddies, and is not limited to riverine floodplains. We thus adopt a broad definition of the term 'floodplains' in this paper, encompassing other inundated surfaces, such as inland wetlands and flooded areas that are not adjacent to rivers, including lacustrine and palustrine flood zones and rice paddies. We use 'floodplains' over the more inclusive expression 'wetlands' as our focus is actual inundation (flooding), whereas wetlands also include peatlands or wet soils that may not be represented in the GIEMS-D15 inundation map.

The goal of this study is to provide a first-order estimate of the spatial extent of human use and appropriation of floodplains and inundated areas in terms of settlements, infrastructure, and agriculture. The results are intended to inform future assessments of benefits or risks that are driven by the spatial co-location of human development and floodplains, such as the provision of ecosystem services, vulnerability to climate change, and flood risk.

2. Methods

2.1. Data

2.1.1. Global inundation extent: GIEMS-D15

The GIEMS-D15 dataset (Global Inundation Extent from Multi-Satellites – Downscaled to 15 arc-seconds; Fluet-Chouinard et al., 2015) was produced using geospatial downscaling techniques to convert monthly inundation observations from multiple satellites within the 12-year period of 1993 to 2004 (Prigent et al., 2007; Papa et al., 2010) from the coarse original resolution of 25 km cells to a finer grid resolution of 15 arc-second pixels (~500 m at the equator) based on topographic indices. GIEMS-D15 represents both natural and artificial inundated surfaces, including rice paddies. Despite being a downscaled product, we chose GIEMS-D15 because (1) its representation of flooded vegetation is more comprehensive than optical remote sensing products that only include open water (Aires et al., 2017), and (2) its aggregated temporal dimension allows for differentiated overlays. GIEMS-D15 distinguishes three temporal states, or 'zones', of inundation (see Fig. 1):

1) The 'mean annual minimum,' here referred to as the zone of *regular* inundation, is indicative of the extent which consistently experiences inundation (or wet soils) throughout the average year.
2) The 'mean annual maximum,' here referred to as the zone of *seasonal* inundation, generally depicts the water extent during the wettest month of the year.
3) The 'long-term maximum,' here referred to as the zone of *infrequent* inundation, is reached during inter-annual flood events. The specific return-period of this inundation extent, however, is not defined in the source data (Fluet-Chouinard et al., 2015).

The overall land area in inundation zones is relatively evenly distributed between the regular (36.2%), seasonal (31.3%), and infrequent (32.4%) zones. The GIEMS-D15 dataset does not explicitly account for human structures (e.g., levees and dams) that protect areas from flooding in its downscaling; but the control of flooding by these structures should manifest as the absence of flooding in the input satellite imagery and thus within the GIEMS-D15 inundation estimates. Also, due to its aggregated temporal dimension, GIEMS-D15 does not represent individual flood events (e.g., stormwater floods at the local scale). Inundation in coastal regions is prone to overestimation, and inland flooding is not properly distinguished from coastal inundation in GIEMS-D15 (Fluet-Chouinard et al., 2015). To avoid bias effects from marine water signals, only inland flooding was considered in this assessment, defined as inundation that occurs more than 25 km (or one original GIEMS grid cell) inland from the coastline.

2.1.2. Global population: WorldPop

WorldPop (WorldPop and CIESIN, 2019) provides global population data at 3 arc-second resolution (~90 m at the equator) for the years 2000–2020. WorldPop uses population counts from the most recent and highest-resolution census information available as inputs, supplemented by estimates from satellite imagery and household surveys where census data were incomplete or out-of-date. The population counts were adjusted based on rural and urban growth rates to produce annual estimates (Stevens et al., 2015), and were disaggregated to the 3 arc-second resolution using Random Forest modelling, based on a weighting surface produced from a combination of ancillary datasets, including topography, settlements, road networks, nightlights, climate, and waterways (Lloyd et al., 2017). The methods used to disaggregate the data are less accurate in rural areas, as small settlements (i.e., less than a few hundred meters across) are not detected. Additionally, the weighting surface methodology produces non-zero values for all pixels, meaning that census population counts are distributed to all pixels in a region. These weaknesses lead to overly homogenous results in rural areas; however, they have little effect on urban population distributions (Smith et al., 2019).

For our assessment, we aggregated the WorldPop population counts per pixel for the year 2015 to match the resolution of GIEMS-D15. We also produced a layer of urban population counts by overlaying the population grid with an urban extent grid (see *2.1.3*); all non-urban population was considered rural.

2.1.3. Global urban extent: GHSL

The Global Human Settlement Layer (GHSL) database provides global spatial layers of human population and settlement patterns for multiple time periods (Florczyk et al., 2019). GHSL consist of: built-up area maps derived from Landsat data; population grids derived from Gridded Population of the World v4.10 (GPW) data, disaggregated from census information based on built-up area distributions; and Settlement Model (GHS-SMOD) grids displaying the degree of urbanization, derived from the built-up area cluster size and population density obtained from the previous two layers.

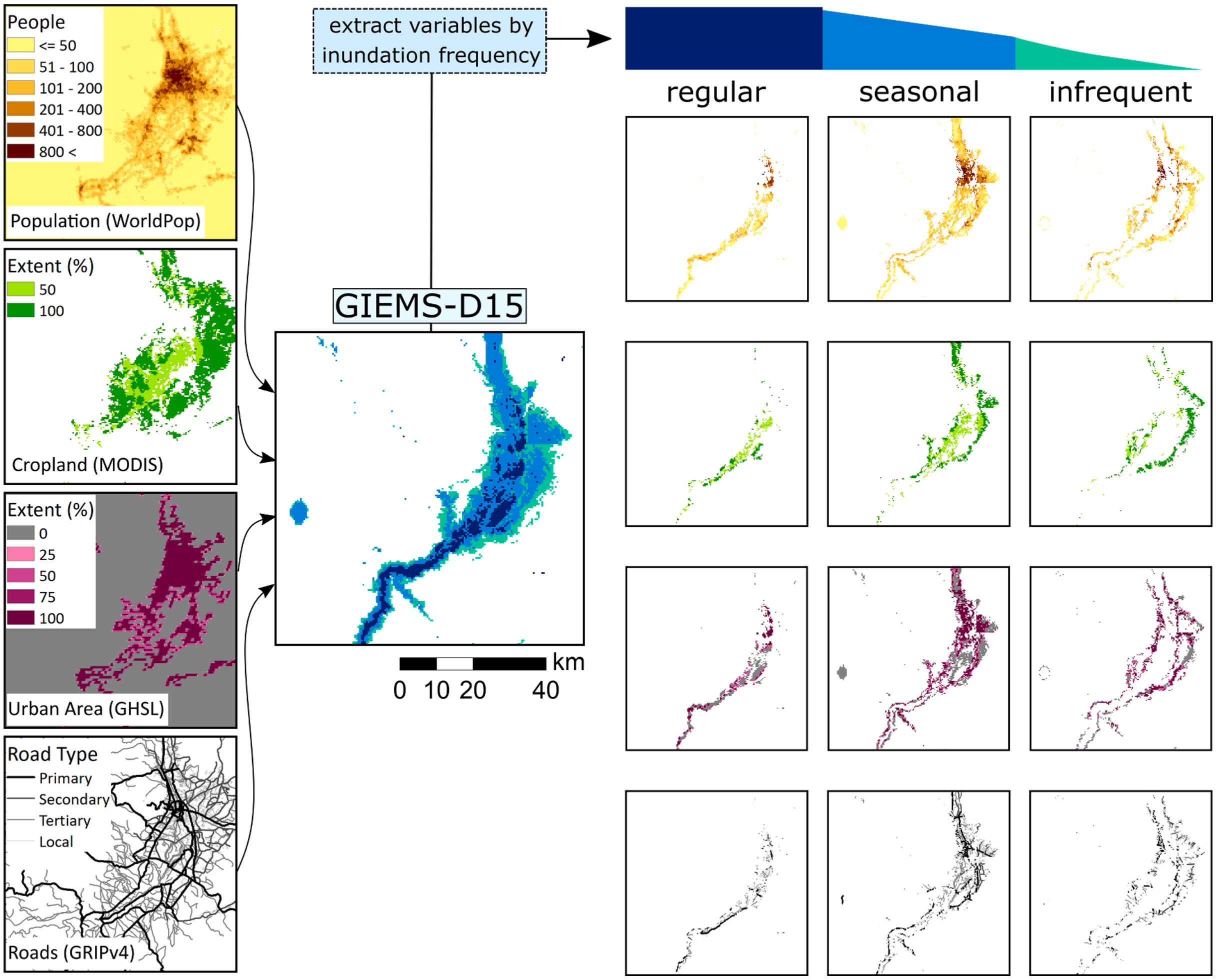

Fig. 1. Schematic of the extraction of thematic data (left column) performed via an overlay with the GIEMS-D15 inundation zones (center) in Chiang Mai region, Thailand; the example shown here displays the presence of each variable within each inundation zone (three columns on right).

We derived urban extents from the 1-km resolution GHS-SMOD layer (Pesaresi et al., 2019) for 2015 by extracting all pixels that were classified as high- or low-density urban clusters; all other areas (unpopulated and rural pixels) were excluded.

2.1.4. Global cropland: MODIS land cover

The Collection 6 MODIS Land Cover Type Product (MCD12Q1; Friedl and Sulla-Menashe, 2019) provides global maps of land cover at 15 arc-second resolution produced at an annual timestep derived from Moderate Resolution Imaging Spectroradiometer (MODIS) data. Land cover layers were produced for each year by performing a supervised classification on a full year of gap-filled 8-day MODIS Nadir BRDF-Adjusted Reflectance data, using a hierarchically nested classification scheme which allowed for the production of multiple legends. One known weakness of this data collection occurs in areas of the tropics where field sizes are small relative to the MODIS pixel size and cropland is sometimes misclassified as natural vegetation (Sulla-Menashe and Friedl, 2018).

We used the MODIS land cover data for the year 2015 in WGS84 projection and selected the FAO Land Cover Classification System (LCCS2) legend as the most detailed classification of cropland. We considered three cropland classes: the class *Cropland (greater than 60% cultivated)* was assumed to be entirely used as cropland, while the two classes *Forest/Cropland Mosaic (40–60% cultivated)* and *Natural Herbaceous/Cropland Mosaic (40–60% cultivated)* were both assumed to be half cropland.

2.1.5. Global roads: GRIPv4

The Global Roads Inventory Project version 4 (GRIPv4; Meijer et al., 2018) is a harmonized global dataset comprising 21.6 million km of road networks. GRIPv4 was compiled from national and international data from both NGOs and crowd-sourced initiatives, such as OpenStreetMap, with the aim of reducing fragmentation and regional inconsistencies compared to previous road data. Input data sources were required to have a maximum positional accuracy of 500 m and a scale ranging from 1:100,000 to 1:500,000. We obtained the GRIPv4 dataset in vector format with attribute information classifying each line segment into one of five road types: (1) highways, (2) primary roads, (3) secondary roads, (4) tertiary roads, and (5) local roads. Class 5 shows evidence of underprediction as local roads are primarily derived from crowd-sourced datasets, and thus, display a spatial bias with coverage concentrated in more developed regions and urbanized areas (Meijer et al., 2018).

2.2. Calculations and comparisons

To estimate human dependence and exposure upon flooded areas, we calculated the extent of multiple anthropogenic variables within each inundation zone from GIEMS-D15 (i.e., regular, seasonal, and infrequent, as well as non-flooded). The inland inundation zones were used to derive the proportions of total, urban, and rural populations; total, urban, and cropland areal extents; and road length within and outside of flooded areas. The raster-based population, urban, and cropland grids were overlaid with the inundation zones to calculate total area and population values for each variable within each zone. The road length calculations were performed in vector format by clipping the road lines to each inundation zone and aggregating their total lengths per zone.

Finally, we compared our human dependence and exposure results to estimates found in literature, flood exposure models, and empirical databases of reported flood impacts. We delineated national boundaries using the Global ADMinistrative areas database (GADM, 2010). Countries were grouped into twelve continental regions following the UN Statistics Division composition of geographical regions (UNSD, 2020), with some of our own modifications similar to those suggested by Kummu et al. (2010) to better represent regions with distinct patterns of water resource and population distribution: North, Central, and South America, Europe, Middle East, North and Sub-Saharan Africa, North, East, Southeast, and South Asia, and Oceania (see Supplementary File for complete country list associated with these sub-regions).

3. Results

Detailed results for all inundation zones, delineated by country and continental region, can be found in the Supplementary File.

3.1. Population

Of the 5.8 billion people living within the region of analysis in 2015 (i.e., all ice-free land excluding areas within 25 km of the coast), 2.0 billion people are located within one of the three inundation zones, representing 35% of global population (Table 1). The proportion of the world's urban population within inundated areas is higher than the proportion of the rural population (38% and 32%, respectively). Given that 14.1 million km^2, or 12% of the total assessed land area are classified as inundated surfaces, the population density in inundated areas is approximately three-times higher than if people were equally distributed across the global land surface. Globally, urban and rural populations are predominantly located within the seasonal inundation zone with a respective 60%, 57%, and 62% of the total, urban, and rural populations in floodplains residing within this zone (Fig. 2).

The percentage of the human population living in inundated areas varies considerably across regions, ranging from 8% in Oceania to 55% and 57% in Southeast and South Asia, respectively. While all continental regions show a higher concentration of urban population in inundation zones relative to rural (Table 1), the highest differences between the two occur in Southeast Asia (67% versus 45%), East Asia (51% versus 31%), and North Africa (34% versus 19%).

South and East Asia have the largest total floodplain populations but with different distributions: 362 million urbanites in East Asia and 561 million rural South Asians reside in inundation zones. The high concentration in these regions is likely caused by co-location of large population numbers within lowland rice growing areas and large river deltas, as well as rapid economic growth, land-use change, and dense urban development in former wetland and riverine floodplain areas. It is important to note that these high population counts are a strong driver of global averages.

The regional population concentrations within the inundation zones exceed the respective expected population density if people were equally distributed across the region for total, urban, and rural populations (grey shading in Table 1 and exceedance of dashed line in Fig. 3), with the exception of rural populations in North and South America.

3.2. Urban settlements

The global urban extent in our study region amounts to 1.74 million km^2, or 1.4% of the analyzed global inland area (Table 2). A total of 35% of global urban area falls within the inundation zones, thus like population, urban areas are about three times more concentrated within floodplain regions than outside. This exposes costly infrastructure and

Table 1
Total, urban, and rural population distributions within inundation zones (floodplains) by sub-region. The percentage of land area in floodplains by sub-region serves as a benchmark for assessing trends in population distributions; grey shaded percentages exceed the benchmark, indicating preferential occurrence of populations in floodplains. Regional floodplain coverage varies from as low as 3% for North Africa to as high as 30% for South Asia, with a global average of 12%. Note that the analyzed land area excludes a 25 km buffer at the coast.

	Land area			Total population			Urban population				Rural population			
	total	*in floodplain*		*total*	*in floodplain*		*total*		*in floodplain*		*total*		*in floodplain*	
	10^6 km^2	10^6 km^2	*(%)*	10^6	10^6	*(%)*	10^6	*(% of total)*	10^6	*(%)*	10^6	*(% of total)*	10^6	*(%)*
North America	17.1	3.6	*(21.2)*	268.8	59.3	*(22.1)*	180.4	*(67.1)*	44.6	*(24.7)*	88.4	*(32.9)*	14.7	*(16.6)*
Central America	2.2	0.2	*(7.8)*	153.1	14.1	*(9.2)*	101.8	*(66.5)*	9.8	*(9.6)*	51.3	*(33.5)*	4.3	*(8.3)*
South America	16.8	1.9	*(11.2)*	304.9	35.7	*(11.7)*	187.2	*(61.4)*	22.6	*(12.1)*	117.7	*(38.6)*	13.1	*(11.1)*
Europe	9.1	0.9	*(9.5)*	574.4	97.4	*(17.0)*	345.8	*(60.2)*	72.2	*(20.9)*	228.6	*(39.8)*	25.2	*(11.0)*
Middle East	4.9	0.3	*(7.0)*	193.2	40.2	*(20.8)*	77.7	*(40.2)*	17.4	*(22.4)*	115.6	*(59.8)*	22.9	*(19.8)*
North Africa	7.4	0.2	*(3.3)*	161.6	45.7	*(28.3)*	95.9	*(59.4)*	33.0	*(34.4)*	65.7	*(40.6)*	12.7	*(19.3)*
Sub-Saharan Africa	21.6	1.6	*(7.3)*	831.2	93.9	*(11.3)*	239.9	*(28.9)*	29.7	*(12.4)*	591.3	*(71.1)*	64.2	*(10.9)*
North Asia	16.5	1.5	*(9.3)*	115.2	12.2	*(10.6)*	44.9	*(39.0)*	5.0	*(11.0)*	70.3	*(61.0)*	7.3	*(10.4)*
East Asia	11.1	1.4	*(12.2)*	1276.4	536.0	*(42.0)*	714.8	*(56.0)*	361.7	*(50.6)*	561.6	*(44.0)*	174.3	*(31.0)*
Southeast Asia	3.2	0.7	*(21.9)*	324.1	178.3	*(55.0)*	151.9	*(46.9)*	101.1	*(66.5)*	172.2	*(53.1)*	77.2	*(44.8)*
South Asia	4.8	1.5	*(30.2)*	1549.4	879.5	*(56.8)*	540.3	*(34.9)*	318.1	*(58.9)*	1009.1	*(65.1)*	561.4	*(55.6)*
Oceania	7.6	0.4	*(4.9)*	11.0	1.0	*(8.1)*	3.4	*(31.1)*	0.3	*(8.5)*	7.6	*(68.9)*	0.7	*(8.0)*
Global	**122.4**	**14.1**	***(11.6)***	**5763.4**	**1993.3**	***(34.6)***	**2684.0**	***(46.6)***	**1015.4**	***(37.8)***	**3079.4**	***(53.4)***	**977.9**	***(31.8)***

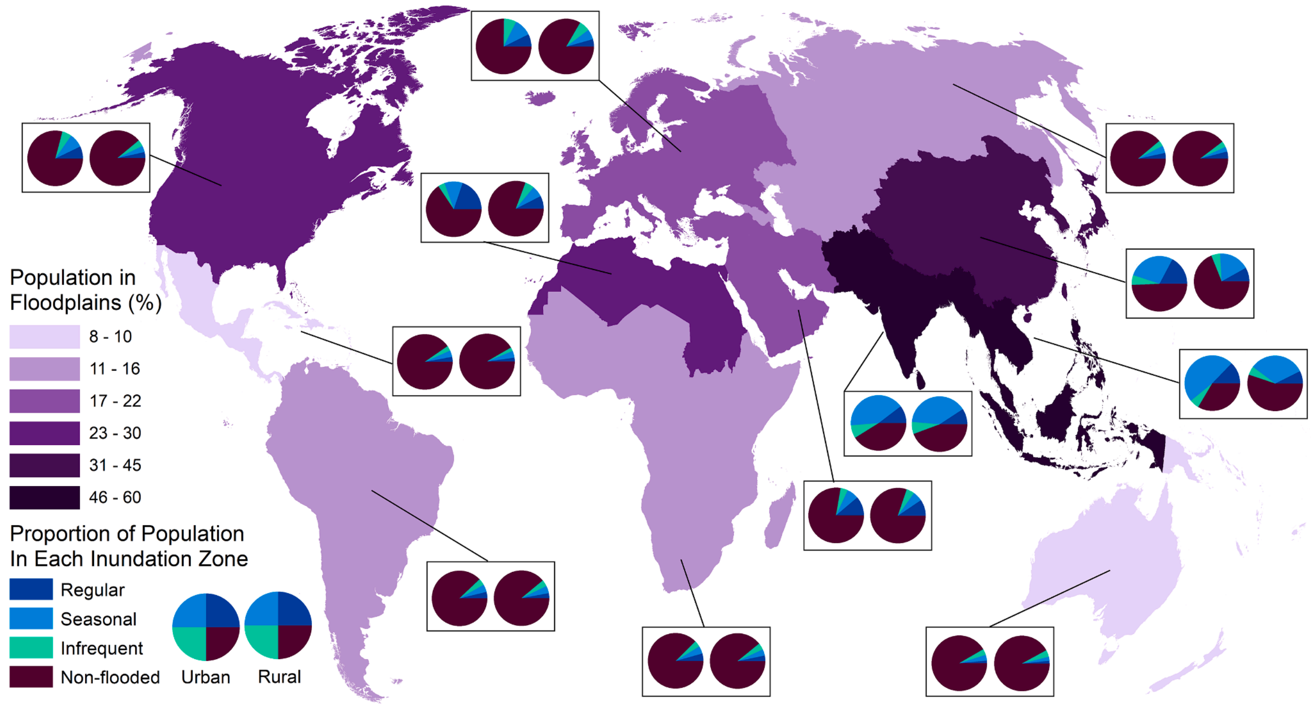

Fig. 2. Distribution of population within each inundation zone displayed in pie charts for both urban (left) and rural (right) populations for each of the twelve continental regions. The base map indicates the percentage of the region's total population that is located in the maximum floodplain extent (i.e., within the combined regular, seasonal, and infrequent inundation zones).

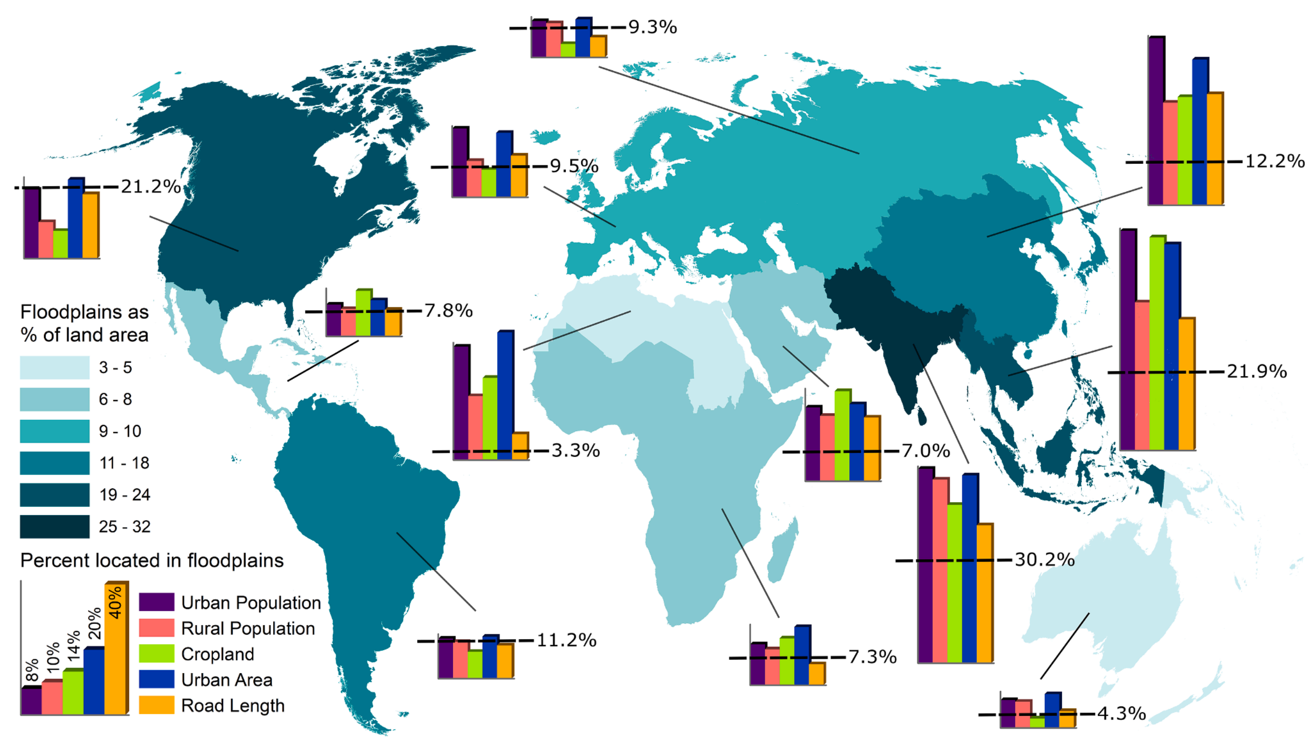

Fig. 3. Percentage of urban and rural populations, croplands, urban extent, and road length located within inundated areas, displayed for each of the twelve continental regions. Each regional bar chart shows a dashed line indicating the percentage of the region's total land area that is located within inundated areas; values exceeding this line indicate preferential usage of inundated areas for human appropriation.

Table 2
Total, urban, and cropland area and road length within inundation zones (floodplains) by sub-region. The percentage of land area in floodplains by sub-region serves as a benchmark for assessing trends in urban, cropland, and road distributions; grey shaded percentages exceed the benchmark, indicating preferential occurrence of urban areas, cropland areas, and roads in floodplains. Regional floodplain coverage varies from as low as 3% for North Africa to as high as 30% for South Asia, with a global average of 12%. Note that the analyzed land area excludes a 25 km buffer at the coast.

	Land area			Urban area				Cropland area				Road length		
	total	*in floodplain*		*total*		*in floodplain*		*total*		*in floodplain*		*total*	*in floodplain*	
	10^6 km²	10^6 km²	*(%)*	10^5 km²	*(% of land)*	10^5 km²	*(%)*	10^5 km²	*(% of land)*	10^5 km²	*(%)*	10^5 km	10^5 km	*(%)*
North America	17.1	3.6	*(21.2)*	1.6	*(0.9)*	0.4	*(23.9)*	19.0	*(11.1)*	4.3	*(22.5)*	26.7	5.2	*(19.6)*
Central America	2.2	0.2	*(7.8)*	0.4	*(1.9)*	0.0	*(11.0)*	1.3	*(6.3)*	0.2	*(13.8)*	7.9	0.6	*(8.1)*
South America	16.8	1.9	*(11.2)*	0.8	*(0.5)*	0.1	*(12.7)*	7.5	*(4.4)*	0.6	*(8.1)*	22.5	2.3	*(10.1)*
Europe	9.1	0.9	*(9.5)*	2.4	*(2.6)*	0.5	*(19.6)*	25.5	*(28.2)*	2.1	*(8.4)*	34.9	4.4	*(12.6)*
Middle East	4.9	0.3	*(7.0)*	0.5	*(1.0)*	0.1	*(23.3)*	1.7	*(3.4)*	0.5	*(27.3)*	5.1	1.0	*(19.3)*
North Africa	7.4	0.2	*(3.3)*	0.5	*(0.6)*	0.2	*(38.7)*	2.3	*(3.1)*	0.6	*(24.9)*	3.3	0.3	*(7.9)*
Sub-Saharan Africa	21.6	1.6	*(7.3)*	2.3	*(1.0)*	0.4	*(17.6)*	11.4	*(5.3)*	1.6	*(14.2)*	21.0	1.3	*(6.3)*
North Asia	16.5	1.5	*(9.3)*	0.4	*(0.3)*	0.0	*(11.5)*	5.2	*(3.2)*	0.2	*(4.1)*	8.7	0.5	*(6.1)*
East Asia	11.1	1.4	*(12.2)*	4.4	*(3.9)*	1.9	*(44.1)*	13.2	*(11.9)*	4.3	*(32.8)*	21.8	7.4	*(33.7)*
Southeast Asia	3.2	0.7	*(21.9)*	1.1	*(3.4)*	0.7	*(62.5)*	4.6	*(14.4)*	3.0	*(64.6)*	8.2	3.3	*(39.7)*
South Asia	4.8	1.5	*(30.2)*	3.1	*(6.3)*	1.7	*(56.9)*	21.7	*(45.0)*	10.4	*(48.0)*	15.3	6.4	*(41.8)*
Oceania	7.6	0.4	*(4.9)*	0.0	*(0.1)*	0.0	*(10.3)*	2.9	*(3.7)*	0.1	*(2.9)*	5.5	0.3	*(5.1)*
Global	**122.4**	**14.1**	***(11.6)***	**17.4**	***(1.4)***	**6.1**	***(35.0)***	**116.4**	***(9.5)***	**27.9**	***(24.0)***	**181.1**	**33.0**	***(18.2)***

puts any urban expansion at risk to future changes in inundation patterns. The percentage of urbanization within inundation zones varies across continents: Oceania displays the smallest proportion at 9%, compared to proportions of 57% and 63% for South and Southeast Asia. Importantly, all continental regions show a preferential location of urban areas within flood-prone areas (grey shades in Table 2 and exceedance of dashed line in Fig. 3).

Urban areas that fall inside inundation zones tend to be concentrated in the seasonal zone with 53% of urban inundated areas found in this zone, compared to 31% in the regular, and 16% in the infrequent zone.

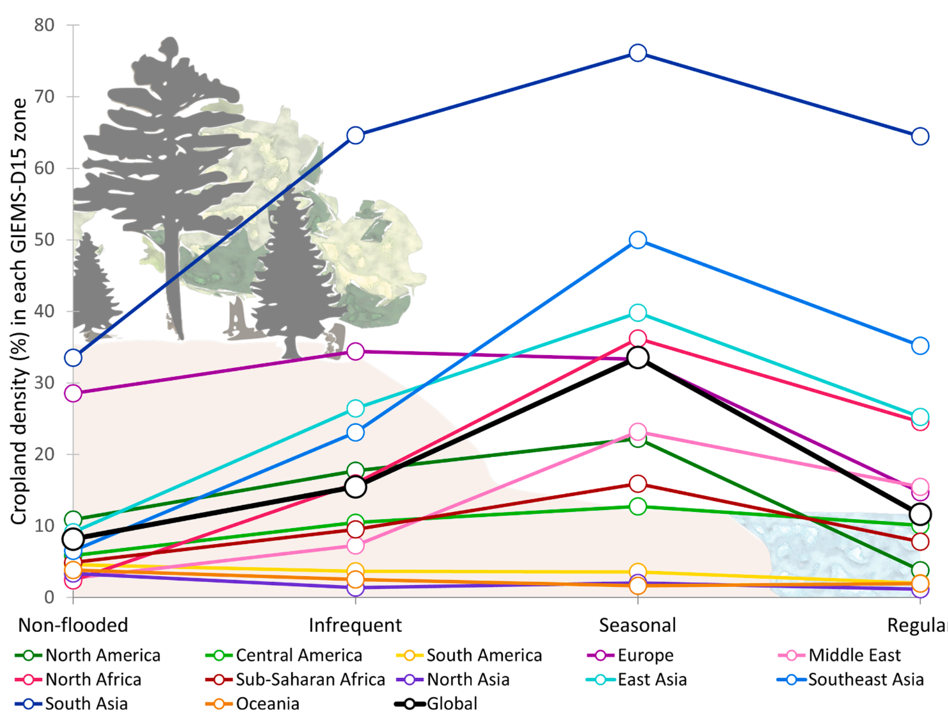

Fig. 4. Cropland density in each inundation zone (including non-flooded), calculated as the ratio between cropland area and total land area in each zone. Lines between points are displayed to better visualize differences across categorical inundation zones.

3.3. Agriculture

Globally, 24% of the world's croplands lie within floodplains and inundated areas (Table 2), which suggests a disproportionate dependence—and also exposure—of croplands to inundation zones. Southeast Asia has the highest percentage of croplands (65%) in inundated areas, followed by South and East Asia, North Africa, and the Middle East, which have 25–50% of croplands in inundated areas. In contrast to this global pattern, however, croplands are disproportionately outside of the inundation zones (not shaded in Table 2) in South America, Europe, North Asia, and Oceania, possibly indicating a dominance of rainfed agriculture or groundwater use (in Oceania) in these regions.

Of the croplands within inundated areas, a majority of 53% are found in the seasonally inundated zone, followed by 25% in the infrequent zone, and 21% in the regular zone, respectively. This zonal preference is mirrored in the cropland density of most continental sub-regions (Fig. 4), showing a peak in the seasonal zone. Notable exceptions are Europe, Oceania, and South America, where the peak in cropland density is observed in the infrequent inundation zone.

3.4. Road infrastructure

Our results show that 18% of global roads, or 3.3 million km of length, are located in floodplains and inundated areas (Table 3), indicating that road infrastructure also tends to disproportionally exist within floodplains. All five road classes display this preferential co-location within floodplains, being strongest for highways (25%) followed by local roads (21%), primary roads (20%), secondary roads (18%), and tertiary roads (16%). The global trend of preferential road construction in inundated areas is mirrored in most continental regions (grey shading in Table 2 and exceedance of dashed line in Fig. 3), with the exceptions of North America, South America, Sub-Saharan Africa, and North Asia.

3.5. Comparisons

3.5.1. Comparisons with population and urban exposure model estimates

We made extensive efforts to compare our findings related to populations, urban areas, and roads to estimates from prior, peer-reviewed studies, as well as with reported impacts. An overview of the studies used for comparisons and their results is provided in Table 4.

Dilley et al. (2005) estimated that more than 33% of the world's land area is flood-prone, with the *most* flood-prone areas occupying about 9% of global land area; our estimate of total inundated area (12%) falls on the lower end of this range. Approximately 82% of the world's population was found to be flood-prone by Dilley et al. (2005) with more than 2 billion people (38% of total global population in the year 2000, excluding grid cells with fewer than 105 residents) occupying the *most* flood-prone areas on a global scale. This estimate is similar to our finding of 2.0 billion people (35% of analyzed population in 2015) living in inundated areas. It should be noted that our estimate refers only to inland inundation (i.e., excluding a 25 km coastal buffer inhabited by 1.6 billion people), while Dilley et al. (2005) assessed both inland and coastal flooding. The population presently exposed to coastal flooding, defined as those living below the annual tidal flood levels, is estimated as high as 250 million people (Kulp and Strauss, 2019).

Table 3
Global road length distribution by road class within inundation zones (floodplains). Note that the analyzed land area excludes a 25 km buffer at the coast.

Road type	Road length		
	total	*in floodplain*	
	10^3 km	10^3 km	(%)
Highways	625	156	*(25.0)*
Primary roads	2,116	431	*(20.4)*
Secondary roads	4,297	755	*(17.6)*
Tertiary roads	7,496	1,204	*(16.1)*
Local roads	3,576	750	*(21.0)*
Total	**18,111**	**3,296**	***(18.2)***

Kummu et al. (2011) estimated that 3.3 billion, or 50% of the global population in 2007, lived within 3 km of an inland waterbody, and 90% (or 5.9 billion people) within 10 km. They also found that the median distance to water was about the same for rural, urban, and peri-urban populations. Our results fall generally within the lower limit of this envelope, although Kummu et al. (2011) did not explicitly distinguish inundation areas but only considered distance from existing freshwater bodies. We find that urban populations have a stronger tendency to reside in inundation zones than rural populations.

Jongman et al. (2012) quantified the number of people exposed to river floods with a 1-in-100-year return period between 1970 and 2050 at a global scale. For 2010, the total population exposed amounted to 805 million, i.e. less than half of the 2.0 billion found to be living in inundated areas in our study. These results are not directly comparable, however, due to the different source data and methodologies used. Table 5 shows a comparison of results for five select flood-prone countries (and globally), broken down into the three GIEMS-D15 inundation zones. The regular inundation zone includes many permanent natural wetlands and areas of widespread rice cultivation, which are not likely to be affected by riverine floods as modeled by Jongman et al. (2012). Our estimates for the seasonal zone, which are closest but still exceed those by Jongman et al. (2012), may also include some wetland areas that are not directly exposed to river floods. Finally, the infrequent inundation zone may include floods that are more extreme than 1-in-100-year events; however, since our inundation zones are based on a 12-year satellite time series (albeit combined with a static map), a 1-in-100-year river flood event was likely not observed for most of the world. Overall, our larger numbers are presumed to be a result of including any kind of inundation, including heavily populated irrigated rice regions co-located in inundation zones (with beneficial dependence), rather than strictly 1-in-100-year river floods.

UNDP (2004) estimated that about 196 million people in more than 90 countries are exposed to catastrophic flooding. While our study does not distinguish 'catastrophic' flooding from general inundation, it may be argued that those living in areas that are rarely inundated are particularly vulnerable to extreme inundation, as they may be less prepared for unexpected flood events. This would be most similar to the infrequent zone in our study, in which we found a total of 290.2 million people for these 90 countries, or 314.6 million globally.

Balk et al. (2012) evaluated urban populations at flood risk across all Asian countries. Their study indicated Cambodia (76%), Vietnam (39%), Bangladesh (36%), Laos (34%), and Thailand (29%) to have the largest proportions of urban populations at risk of inland flooding. Our results show the same 5 countries, plus Myanmar, to have the highest ratios of urban populations within all inundation zones across Asia, albeit at consistently higher proportions (93%, 85%, 99%, 77%, and 90%, respectively). We attribute these rather substantial differences primarily to varying definitions and perspectives between our studies: Balk et al. (2012) considered only exposure to extreme river flooding events (~1-in-50-year floods), while our study includes any kind of inundation, including semi-regular to permanent flooding of rice paddies or large river deltas, which can be considered beneficial rather than a risk. Despite these differences, both studies highlight the same countries in Asia as facing severe risks and/or showing strong dependence regarding their floodplain and wetland environments and the services they provide.

Using stage-damage function inundation models, Ward et al. (2013) estimated the annual expected impacts of inland flooding, including: 169 million people exposed (or 2.5% of global population); 1.4 trillion USD exposed (representing 2.2% of global GDP); affected agriculture valued at 75 billion USD (0.1% of global GDP); urban damage potential at 834 billion USD (1.3% of global GDP); and exposed urban assets at 5.3

Table 4
Comparative summary of exposed population estimates found in literature. Note that sources use different metrics and methods, as well as varying spatial scales.

Study	Geographic scope	Includes	Metric	Population	Our Study
Dilley et al. (2005)	Global and subnational scales (per grid cell)	Six major hazards + flood risk of population and GDP	Historic mortality and economic losses, based on DFO reports of extreme flood events	• 4.3 billion (82%) flood-prone • 2 billion (38%) most flood-prone	• 11.6% inundated area • 2.0 billion people living in all inundation zones
Kummu et al. (2011)	Global	Inland inundation related to urban and rural population	Population at different distances to freshwater bodies	• 3.3 billion (50%) ≤ 3 km from freshwater body • 5.9 billion (90%) within 10 km	• 11.6% inundated area • 2.0 billion people living in all inundation zones
Jongman et al. (2012)	Global and per country	Inland flood risk of population	Hydrological modeling and 1-in-100-year flood records	• 805 million exposed to floods	• 2.0 billion people living in all inundation zones
UNDP (2004)	Global and per country	Risk of death by country that includes flood exposure	Mortality rate from reported flood events	• 196 million in greater than 90 countries exposed to catastrophic flooding	• Infrequent inundation zone in the same 90 countries: 290 million
Balk et al. (2012)	All Asian countries (for our comparisons, we selected their 5 countries that had the highest percentage of urban population exposed)	Coastal and inland flood risk (comparisons to our study include inland flood risk only)	Modeled flood extents (representing ~1-in-50-year events); urban population only	• Main countries: Bangladesh (36%), Cambodia (76%), Laos (34%), Thailand (29%), Vietnam (39%)	• Urban population living in all inundation zones: Bangladesh (99%), Cambodia (93%), Laos (77%), Thailand (90%), Vietnam (85%)
Ward et al. (2013)	Global	Inland flood risk of population, GDP, agricultural value, and land use	Stage-damage function inundation model	• 169 million people exposed	• 2.0 billion people living in all inundation zones
Smith et al. (2019)	18 developing countries, including 4 landlocked (Burkina Faso, Malawi, Rwanda, Uganda) and 7 countries with greater than 80% of population inland (4 landlocked plus Cambodia, Mexico, Tanzania)	Population at-risk from fluvial or pluvial flooding	High resolution (30 m) population density map and 90 m resolution hydrodynamic inundation model	• 101 million exposed to 1-in-100-year flood event across 18 developing countries • 40 million exposed in the 7 countries with greater than 80% of population inland • 5.6 million exposed in the 4 landlocked countries	• 60 million people living in all inundation zones across the same 18 countries (excluding a 25 km coastal buffer) • 38 million living in all inundation zones in the 7 countries with greater than 80% of population inland • 11 million living in all inundation zones in the 4 landlocked countries

Table 5
Population comparisons between exposure estimates made by Jongman et al. (2012) and our results of people living in different inundation zones for select flood-prone countries and globally. Population estimates expressed in millions of people.

	Jongman et al. (2012)	Regular zone (5.1 mill. km^2)	Seasonal zone (4.4 mill. km^2)	Infrequent zone (4.6 mill. km^2)	All flood zones (14.1 mill. km^2)
Bangladesh	76.0	23.8	95.6	2.5	121.8
China	173.0	152.8	279.3	66.1	498.1
India	195.0	106.3	464.7	92.5	663.4
U.S.A.	26.0	13.1	20.1	15.8	49.0
Vietnam	29.0	8.3	34.5	2.8	45.6
Global	**805.0**	**492.2**	**1186.5**	**314.6**	**1993.3**

trillion USD (8.2% of global GDP). Our estimate of global population exposure far exceeds that of Ward et al. (2013), albeit our data, definitions, and methods differ widely. While we do not include economic damage assessments in this study, the high economic exposure of urban areas, assets, and agriculture (Ward et al., 2013) underscores the importance of quantifying global floodplain dependence and exposure in our work.

Güneralp et al. (2015) found that 30% of global urban extent in the year 2000 was located in high-frequency flood zones. This is similar to our findings that place 35% of urban extent in any of the inundation zones, and 29% in the regular or seasonal zones that experience higher frequencies of inundation. Moreover, Güneralp et al. (2015) found the greatest percentage of urban extent in flood zones within South Asia (69%), India (52%), and Southeast Asia (49%). Our continental breakdown similarly identifies South and Southeast Asia as having the highest percentages of urban area in inundation zones (63% and 57%, respectively).

Koks et al. (2019) analyzed the global extent of roads and railways exposed to natural hazards. They found that 27% of transportation infrastructure was exposed to one or more hazards with a 1-in-250-year return period; and that 73% of the expected damage to infrastructure was caused by surface or river flooding. Furthermore, the study found 7.5% of infrastructure exposed to a 1-in-100-year flood. Koks et al. (2019) considered major flood events and protective design measures, which must be exceeded by a hazard before an asset is exposed; whereas, we determine exposure of roads to any level of inundation. Nonetheless, our estimated 18% of global road length that is within all inundation zones falls within the range of values found in Koks et al. (2019).

3.5.2. Comparison with DFO reporting

We also compared our results to the confirmed number of impacted people reported in the Dartmouth Flood Observatory (DFO) archives

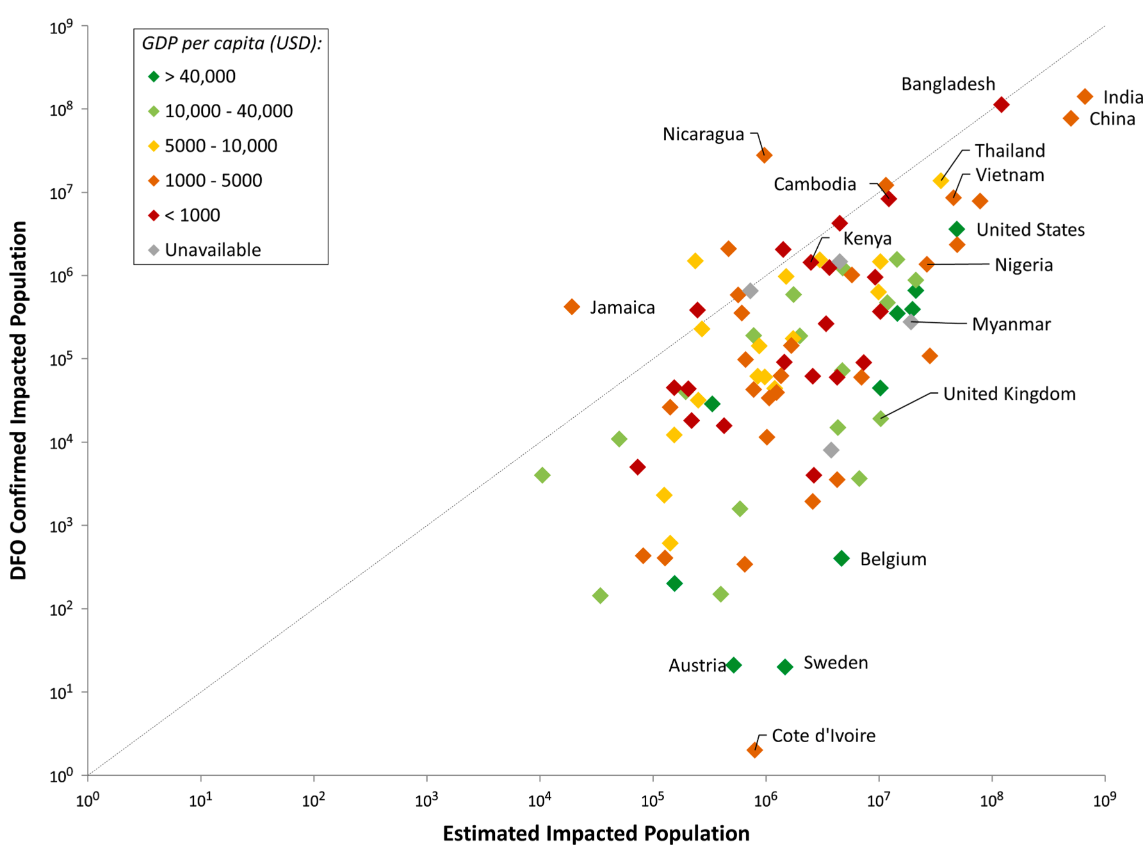

Fig. 5. Confirmed impacted people for large flood events from 1990 to 2005 from the DFO archives compared to our population estimates within all GIEMS-D15 inundation zones (regular, seasonal, and infrequent), color-coded by per capita GDP for 2010. Some countries were removed if DFO assigned zero impacted people yet listed them as secondary/shared country of flooding (including Iraq, Uzbekistan and Mali).

between 1990 and 2005 (approximately the GIEMS-D15 period of record) for each country (Fig. 5). The DFO data represent past and real-time flood events, confirmed deaths, and displaced persons based on flood reports from multiple quantitative and qualitative sources. Overall, there is a moderate alignment between the DFO data and our estimates, although our estimates tend to be higher due to our broader perspective of human floodplain dependence and exposure, which entails more than just catastrophic events. In particular, both the DFO archives of impacted people and our results of population living in inundated areas show the highest total affected populations in India, China, and Bangladesh.

The DFO records single-day major flood events that are not captured in long-term satellite imagery. Also, the DFO data cover coastal floods, which are not well represented by GIEMS-D15, and can explain our underestimations in countries such as Nicaragua and Jamaica.

The number of displaced persons and fatalities can be particularly high in developing countries during flood events due to limited mitigative measures and adaptive capacity. In developed countries, such as Austria and Sweden, the same flood event may impact fewer people due to the presence of flood protection. While our analysis does not consider infrastructure and mitigative practices that may provide flood protection (where present), our estimates tend to better match DFO reported impacts in developing countries compared to developed ones.

3.5.3. *Comparison of dependence on floodplain agriculture*

Limited studies exist for direct comparison of floodplain agriculture dependence. At a global scale, Arnell and Gosling (2016) identified over 1 million km^2, or 7%, of global croplands within flood-prone regions. This is significantly lower than our value of 2.8 million km^2 (24%) of croplands that lie within inundated areas. Arnell and Gosling (2016) produced their results at coarser spatial resolution (0.5 degree) and only considered flooding from large rivers, thus focusing on the exposure to major flood events rather than also including the beneficial dependence of agriculture to regular or seasonal flooding at smaller scales. As such, the findings by Arnell and Gosling (2016) may more closely match the infrequent zone in our study, where we find 6.1% of global cropland extent. As with our results, Arnell and Gosling (2016) found the highest amount of exposed croplands in South Asia.

A recent analysis of irrigated croplands used remotely sensed data, national and sub-national surveys, and climate data to produce a global map of Global Rain-fed, Irrigated, and Paddy Croplands (GRIPC; Salmon et al., 2015) for the year 2005. The map shows 1.29 million km^2 of irrigated or rain-fed paddy areas, which are primarily located in the southern part of Asia. This result is similar to our finding of 1.48 million km^2 of croplands in the regular and seasonal inundation zones of East, South, and Southeast Asia, which we assume are dominated by paddy rice cultivation.

Richter et al. (2010) estimated that a minimum of 3 million people depend on African floodplains for agriculture, including flood recession agriculture and pastoralism; however, they only included specific river basins in certain countries in their study, i.e. Nigeria, Cameroon, Botswana, Ethiopia, Tanzania, Mali, Mauritania, Senegal, and Kenya. For the same countries, we estimate that 13.3 million rural people occupy croplands within inundated areas. These higher population estimates can be expected, as our spatial extent is larger (all basins), and our definition is more inclusive (mapping co-habitation rather than actual dependence on African floodplains). Thus, the results uphold the notion that floodplain and wetland cultivation may broadly be captured by overlaying global gridded data on rural population and cropland extents within inundated areas.

More specifically, Richter et al. (2010) estimated that nearly 34,000 people in the Ngamiland district in Botswana were dependent on the Okavango delta. We estimate that a total rural population of over 68,500 is located within inundated areas in Botswana. About 24,000 of those people are within regular and seasonal inundation zones and may depend on recurrent annual flood patterns. In Nigeria, Richter et al. (2010) only considered the farmers, herders, and fishers dependent upon two particular wetlands, which exceeded 1.5 million people; for the same area, we estimate that nearly 294,000 people are within all inundation zones, indicating that our estimates of floodplain dependence can be exceeded in reality. Richter et al. (2010) also estimated that 1 million Kenyans depended on a single river regime (Tana River basin) for their livelihoods, whereas we estimate that approximately 326,000 people are living within inundated areas in this basin, illustrating that floodplain dependence can go beyond co-habitation of the floodplain itself.

In England and Wales, Hall et al. (2005) estimated that 14,300 km^2 of agricultural land lies within floodplains, whereas we estimate that 8,400 km^2 of croplands are within floodplains for the entire United Kingdom (excluding a 25 km coastal buffer). Hall et al. (2005) also considered annual flood risk, and they placed 4.5 million people in flood-risk zones, or 8.7% of the population in their study area. Annual risk is most similar to our seasonal inundation zone, in which we find 3.9 million people in the United Kingdom, or 6.1% of the total analyzed population.

4. Discussion

Our results provide strong confirmation for the common understanding that humans favor living and farming in floodplains. We found that 35% of human population (2.0 billion people), 35% of urban areas, 24% of croplands, and 18% of roads are located within the 12% of global inland area that are categorized as inundation zones in GIEMS-D15. This preference towards inhabiting, developing, and cultivating inundated areas makes human society particularly reliant on riparian floodplain environments (Costanza et al., 2014). It also indicates a high exposure to potential future changes in this preferred zone of human development, be it due to increased or decreased flood risks or any changes in beneficial ecosystem services. In addition to potential changes in inland flooding, large increases in coastal flooding are projected with sea level rise, as an estimated one billion people live in areas less than 10 m above current high tide lines (Kulp and Strauss, 2019). Despite the distinct processes and impacts of inland and coastal flooding, these results underscore the significant extent to which humans (and their assets) reside in flood-prone regions worldwide.

As global averages can mask regional differences, we also applied a regional assessment of our findings. On a continental scale, floodplains and inundated areas are prominently favored in South and Southeast Asia, which can partly be attributed to widespread wet rice cultivation and floodplain agriculture. Specifically, these regions demonstrate high proportions of their populations in the seasonal inundation zone (i.e., 40% of each region's population), and similar trends are displayed for croplands (31% and 49%, respectively, for South and Southeast Asia), urban area (36% and 45%), and road length (28% and 29%) in this zone. High population and cropland densities in the seasonal inundation zone indicate a strong reliance on specific flooding patterns and/or irrigation. East Asia, North Africa, and the Middle East also display disproportionately high tendencies of co-located populations and agriculture in inundated areas. With the fastest growing population in the world, Africa's overall reliance on floodplains and exposure to risk may significantly grow in the future.

4.1. *Limitations of inundation data*

Our results have inherent errors and uncertainties. Mapping errors and limited spatial accuracy or resolution of the source data can partially explain the difference of our results to other assessments. The spatial distribution of GIEMS-D15 inundation is generated by topographic downscaling and should thus be considered a modeled delineation. As a result of the topographic downscaling process and the 500 m resolution of the inundation data, we find infrastructure and populations located in the regular inundation zone, including large roads as seen in Fig. 1. It is important to note that the regular inundation zone does not represent only permanent open water but rather consistent regional inundation—including irrigated or wet soils—downscaled to the most topographically flood-prone pixels in the region.

GIEMS-D15 represents hydrologically active floodplains during 1993–2004, thus, the population and croplands located in hydrologically inactive floodplains (i.e., in formerly inundated geomorphic formations) are not considered in this study. The regular and seasonal inundation zones of GIEMS-D15 are derived from this 12-year period of observation, while the infrequent zone does not represent a specific flood frequency due to the fusion of GIEMS data with a static wetland map (GLWD; Lehner and Döll, 2004). Despite this limitation, our results can serve as an adequate proxy to identify general exposure to inundation events on both shorter and longer timescales. Given the temporal dimension of our study, the results are not directly comparable to assessments of specific flood return periods (e.g., 1-in-100-year floods). Despite these discrepancies, our results broadly agree with previous estimates, and differences can be reasonably explained by varying definitions, methods, and datasets.

GIEMS-D15 captures all types of inundation, including artificial inundation from irrigated rice paddies. The GIEMS-D15 retrieval is also potentially sensitive to saturated soils, naturally occurring or from other types of agriculture (Prigent et al., 2007). Given this characteristic of GIEMS-D15, it is expected that inundation co-occurs with people and agriculture, particularly within regions of intense rice cultivation. The overlap of inundation and rice culture should not be interpreted as hazardous in these areas, but rather, as an example of agricultural dependence on inundation. Importantly, it is this dependence that drives our findings of preferential development in inundated areas in South, Southeast, and East Asia, and these regional trends in turn affect the global averages. Conversely, the regular inundation zone of GIEMS-D15 includes permanent waterbodies where croplands or population cannot be expected to be found. The inclusion of permanent waterbodies, i.e. lakes and rivers, as flooded areas reduces our percent estimates of land use density in permanently inundated floodplains and wetlands, such as marshlands or rice paddies. Moreover, we include large northern wetland extents, which do not depend on riverine flooding and are located in remote and/or unpopulated areas. The large extent of these regions contributes to our low estimates of development density in inundated areas for North America and North Asia.

We interpret the GIEMS-D15 inundation extent as capturing general surface inundation, with zones representing different frequencies of inundation. However, the levels of inundation recurrence do not predict the degree of dependence or exposure. For instance, regular and seasonal zones are assumed to be more regularly inundated but may not be more vulnerable, as people within these areas may be more adapted or even manage the inundation waters themselves. When flooding in the infrequent zone does occur, the impacts may be more severe. Moreover, our results do not account for implemented measures of flood protection or mitigation. The countries that have experienced high numbers of displaced individuals and fatalities based on DFO records are not necessarily those where we identified the highest floodplain populations. Some developed nations have been less impacted than their levels of inundation exposure would suggest, likely due to advanced adaptive, coping, and mitigative capabilities.

While the comparison between GIEMS-D15 estimates and DFO archives is informative, the utility of these datasets is highly different in nature. Our method attempts to evaluate baseline floodplain use in terms of exposure and dependence but cannot capture short-term or singular flood events and is not designed to pinpoint potentially impacted persons at a certain location, as can be done by the DFO data.

4.2. Uncertainty of population exposed

A recent analysis estimated population exposed to flood risk by overlaying a high-resolution (90 m) hydrodynamic inundation model with new, 30 m population density maps (Smith et al., 2019). The authors compared their results to other estimates that used global population data at coarser resolutions for 18 developing countries and found that the estimates using coarser population data overestimated population exposed to flood risk by 33% on average (and up to 60%).

Specifically, Smith et al. (2019) estimated that 101 million people were located within the risk area for a 1-in-100-year flood event in their study area when using 30 m population data versus 122 million when using alternative 90 m population data (WorldPop) for the same region. They found that the results of population exposure in urban areas were similar regardless of resolution, whereas higher estimates derived from the coarser population data were largely attributable to a higher spread of population across rural areas. Due to our focus on inland inundation (excluding a 25 km coastal buffer), we compared our results to those of Smith et al. (2019) for only those 7 countries with at least 80% of their total population living inland and additionally for the subset of those 4 countries that are fully landlocked (Table 4). For the 7 countries, our estimates of population in all inundation zones compare well with 38 million against the 40 million found in at risk areas by Smith et al. (2019); for the 4 landlocked countries, our estimates are about double at 11.1 million versus 5.6 million, respectively. Our population exposure estimates per country range from less than half to over 2.5 times those of Smith et al. (2019) for the 7 countries; however, much of the larger national-level variation can be attributed to discrepancies in coastal areas.

A part of the observed discrepancies can be attributed to Smith et al. (2019) considering flood risk from fluvial or pluvial flooding only, whereas we consider all population within any type of inundated area. Our inclusion of lacustrine and groundwater-driven wetlands, as well as rice paddies and floodplain agriculture, result in our population estimates being comparatively higher in many regions. Furthermore, our results are not counts of population vulnerable to flood risks of certain frequencies but rather encompass broad human dependence on floodplains through multiple facets, such as reliance on predictable inundation regimes for those who practice flood recession agriculture and fisheries, as well as other floodplain services and benefits, all alongside exposure.

5. Conclusion

The extensive use of wetlands and floodplains for human settlements, infrastructure, and agriculture demonstrates that populations across the world are highly dependent on predictable inundation regimes, as well as potentially exposed to hydrological changes and extreme events. In this study, we evaluated the relationship between human development and floodplains across the world. In contrast to most earlier studies which focused on the exposure, risk, or vulnerabilities caused by flood hazards, we broadened our perspective by adding the positive dependence of humans and agriculture on regular and seasonal flooding to encompass the multiple benefits and challenges of people's interactions with inundated environments. We used the most comprehensive, high-resolution map of global inundation, including saturated soils, to quantify the extent and concentration of human society in floodplains and inundation areas and to verify our general understanding of the importance of these landscapes. We found that about 35% of the global population (2.0 billion people), 35% of urban areas (610,000 km^2), 24% of croplands (2.8 million km^2), and 18% of roads (3.3 million km) are located within actively inundated areas, which only cover about 12% of global land surface. This study extends previous geographic analyses evaluating human proximity to waterbodies (e.g., Kummu et al., 2011) by explicitly considering the role of floodplains in describing these patterns. Limitations of inundation, wetland, and floodplain extent data required assumptions that affect the reliability of our estimates.

The patterns of dependence and exposure of human population and land use to inundation will face additional pressure from rapid urbanization and environmental change in many regions where these trends are most acute. Coupled with our estimates, other moderating variables include large migration into cities, industrialization, and general social and environmental vulnerability, particularly in less-developed countries (Chinowsky et al., 2011). For example, East, Southeast, and South Asia have large floodplain populations and high concentrations of informal urban settlements, which are unlikely to benefit from natural flood regimes or be protected by flood control infrastructure; hence, our estimates indicate that the existing socio-environmental vulnerabilities may be exacerbated by high floodplain exposure of the urban areas in this region.

By evaluating population, development, and croplands within floodplains, we identified priority regions and countries (see Supplementary File) where different coping strategies are urgently needed, including adaptive or mitigative policies to increase the resilience of urban and rural populations, infrastructure, and critical crop-producing areas. These high-level results are intended for use by international organizations and regional policy makers that are concerned with future development strategies, such as the implementation of water and food-related Sustainable Development Goals (SDGs). In practice, however, comprehensive risk and benefit assessments require information that goes beyond the simple accounting of people, infrastructure, or agricultural assets within flood-prone areas: hazard, exposure, vulnerability, and the level of dependence must all be combined to determine best management plans. Quantifying human presence in floodplains is a necessary first step toward characterizing human reliance on present-day conditions. We provide estimates based on standardized data that can inform future assessments of factors, such as vulnerability to land use and climate change, and guide a more comprehensive and local development of advisable mitigation strategies and justifiable adaptation policies to better harness the benefits of floodplains while reducing their risks.

Our global results provide evidence of the enormous extent to which humans have developed interdependencies with floodplains. The complexity of interactions is particularly challenging, as any intentional or inadvertent alteration from the natural flooding cycle can cause diametric effects, such as decreasing the exposure to flood risks at the cost of losing vital floodplain benefits. An innovative policy mindset will thus be required that considers retreat versus adaptation strategies—e.g., the Blue-Green city approach or the Room for the River concept (van Alphen, 2020). Novel solutions may steer away from the goal of active flow regulation and aim instead at coexistence and management within the given inundation regime, as well as the restoration of floodplains to a more natural state that can sustain mutual benefits for humans and nature.

CRediT authorship contribution statement

Rachel Dryden: Conceptualization, Methodology, Writing – original draft, Writing - review & editing. **Mira Anand:** Data curation, Formal analysis, Visualization, Writing – original draft, Writing - review & editing. **Bernhard Lehner:** Conceptualization, Methodology, Supervision, Writing - review & editing. **Etienne Fluet-Chouinard:** Visualization, Writing - review & editing.

Declaration of Competing Interest

The authors declare that they have no known competing financial interests or personal relationships that could have appeared to influence the work reported in this paper.

Acknowledgements

This work was supported by funding from a Discovery Grant by the Natural Sciences and Engineering Research Council of Canada (NSERC-DG; RGPIN/341992).

Appendix A. Supplementary data

Supplementary data to this article can be found online at https://doi.org/10.1016/j.gloenvcha.2021.102370.

References

Acreman, M.C., Riddington, R., Booker, D.J., 2003. Hydrological impacts of floodplain restoration: a case study of the River Cherwell, UK. Hydrol. Earth Syst. Sci. Discuss. 7 (1), 75–85.

Aires, F., Miolane, L., Prigent, C., Pham, B., Fluet-Chouinard, E., Lehner, B., Papa, F., 2017. A global dynamic long-term inundation extent dataset at high spatial resolution derived through downscaling of satellite observations. J. Hydrometeorol. 18 (5), 1305–1325.

Amador-Jimenez, L., Willis, C.J., 2012. Demonstrating a correlation between infrastructure and national development. Int. J. Sustainable Dev. World Ecol. 19 (3), 197–202.

Arnell, N.W., Gosling, S.N., 2016. The impacts of climate change on river flood risk at the global scale. Climatic Change 134 (3), 387–401.

Asada, H., Matsumoto, J., 2009. Effects of rainfall variation on rice production in the Ganges-Brahmaputra Basin. Climate Research 38 (3), 249–260.

Balica, S.F., Douben, N., Wright, N.G., 2009. Flood vulnerability indices at varying spatial scales. Water Science and Technology: A Journal of the International Association on Water Pollution Research 60 (10), 2571–2580. https://doi.org/10.2166/wst.2009.183.

Balk, D., Montgomery, M.R., Liu, Z., 2012. Urbanization and climate change hazards in Asia. Unpublished Report in Proceedings of the International Union for the Scientific Study of Population. Busan, Republic of Korea.

Chan, F.K.S., Griffiths, J.A., Higgitt, D., Xu, S., Zhu, F., Tang, Y.-T., Xu, Y., Thorne, C.R., 2018. "Sponge City" in China—a breakthrough of planning and flood risk management in the urban context. Land use policy 76, 772–778.

Chinowsky, P., Hayles, C., Schweikert, A., Strzepek, N., Strzepek, K., Schlosser, Adam, C., 2011. Climate change: comparative impact on developing and developed countries. Eng. Proj. Organ. J. 1 (1), 67–80.

Costanza, R., de Groot, R., Sutton, P., van der Ploeg, S., Anderson, S.J., Kubiszewski, I., Farber, S., Turner, R.K., 2014. Changes in the global value of ecosystem services. Global Environ. Change 26, 152–158.

Dilley, M., 2005. Natural disaster hotspots: a global risk analysis (Vol. 5). World Bank Publications. Washington D.C.: United States.

Ding, Y., 2014. In: Handbook of Climate Change Mitigation and Adaptation. Springer New York, New York, NY, pp. 1–29. https://doi.org/10.1007/978-1-4614-6431-0_14-2.

Douglas, I., Alam, K., Maghenda, M., Mcdonnell, Y., Mclean, L., Campbell, J., 2008. Unjust waters: climate change, flooding and the urban poor in Africa. Environ. Urbanization 20 (1), 187–205.

Falkenmark, M., Finlayson, M., Gordon, L.J., Bennett, E.M., Chiuta, T.M., Coates, D., Ghosh, N., Gopalakrishnan, M., de Groot, R.S., Jacks, G., Kendy, E., Oyebande, L., Moore, M., Peterson, G.D., Portuguez, J.M., Seesink, K., Tharme, R., Wasson, R., 2007. Agriculture, water, and ecosystems: avoiding the costs of going too far. Retrieved from. http://ageconsearch.umn.edu/bitstream/158130/2/H040199.pdf.

Fluet-Chouinard, E., Lehner, B., Rebelo, L.-M., Papa, F., Hamilton, S.K., 2015. Development of a global inundation map at high spatial resolution from topographic downscaling of coarse-scale remote sensing data. Remote Sens. Environ. 158, 348–361.

Foudi, S., Osés-Eraso, N., Tamayo, I., 2015. Integrated spatial flood risk assessment: The case of Zaragoza. Land Use Policy 42, 278–292.

Fox, J., Ledgerwood, J., 1999. Dry-season flood-recession rice in the Mekong delta: Two thousand years of sustainable agriculture? Asian Perspect. 38 (1), 37–50.

Friedl, M., Sulla-Menashe, D., 2019. MCD12Q1 MODIS/Terra+Aqua Land Cover Type Yearly L3 Global 500m SIN Grid V006 . NASA EOSDIS Land Processes DAAC. Accessed 2019-11-27 from https://doi.org/10.5067/MODIS/MCD12Q1.006.

Florczyk, A.J., Corbane, C., Ehrlich, D., Freire, S., Kemper, T., Maffenini, L., Melchiorri, M., Pesaresi, M., Politis, P., Schiavina, M., Sabo, F., Zanchetta, L., 2019. GHSL Data Package 2019. Luxembourg: Publications Office of the European Union. doi:10.2760/062975 (JRC 117104, EUR 29788 EN).

Global Administrative Areas, 2010. GADM database of Global Administrative Areas, version 2.0. Accessed 15 JUNE 2015. http://www.gadm.org.

Gonçalves, J.R.P., Fontes, J.R.A., de Morais, R.R., de Moura Rocha, M., Moreira Guimarães, L.J., 2010. Sustainable production of grains in Amazonian floodplain. In Proceedings of the 19th World Congress of Soil Science: Soil solutions for a changing world, Brisbane, Australia, 1-6 August 2010. Symposium 1.1. 1 Soil morphology and climate change (pp. 56-59). International Union of Soil Sciences (IUSS), c/o Institut für Bodenforschung, Universität für Bodenkultur.

Güneralp, B., Güneralp, İ., Liu, Y., 2015. Changing global patterns of urban exposure to flood and drought hazards. Global Environ. Change 31, 217–225.

Hall, J.W., Sayers, P.B., Dawson, R.J., 2005. National-scale Assessment of Current and Future Flood Risk in England and Wales. Nat. Hazards 36 (1-2), 147–164.

Hanna, D.E.L., Tomscha, S.A., Ouellet Dallaire, C., Bennett, E.M., Hooftman, D., 2018. A review of riverine ecosystem service quantification: research gaps and recommendations. J. Appl. Ecol. 55 (3), 1299–1311.

Hirabayashi, Y., Kanae, S., 2009. First estimate of the future global population at risk of flooding. Hydrological Research Letters 3, 6–9.

Hirabayashi, Y., Mahendran, R., Koirala, S., Konoshima, L., Yamazaki, D., Watanabe, S., Kim, H., Kanae, S., 2013. Global flood risk under climate change. Nat. Clim. Change 3 (9), 816–821.

IPCC, 2014. Summary for policymakers. In: Climate Change 2014: Impacts,Adaptation, and Vulnerability. Part A: Global and Sectoral Aspects. Contribution of Working Group II to the Fifth Assessment Report of the Intergovernmental Panel on Climate Change [Field, C.B., V.R. Barros, D.J. Dokken, K.J. Mach, M.D. Mastrandrea, T.E. Bilir, M. Chatterjee, K.L. Ebi, Y.O. Estrada, R.C. Genova, B. Girma, E.S. Kissel, A.N. Levy, S. MacCracken, P.R. Mastrandrea, and L.L.White (eds.)]. Cambridge University Press, Cambridge, United Kingdom and New York, NY, USA, pp. 1-32.

Jongman, B., Ward, P.J., Aerts, J.C.J.H., 2012. Global exposure to river and coastal flooding: long term trends and changes. Global Environ. Change 22 (4), 823–835.

Jonkman, S.N., 2005. Global perspectives on loss of human life caused by floods. Nat. Hazards 34 (2), 151–175.

Junk, W.J., An, S., Finlayson, C.M., Gopal, B., Květ, J., Mitchell, S.A., Mitsch, W.J., Robarts, R.D., 2013. Current state of knowledge regarding the world's wetlands and their future under global climate change: a synthesis. Aquat. Sci. 75 (1), 151–167.

Junk, W.J., Bayley, P.B., Sparks, R.E., 1989. The flood pulse concept in river-floodplain systems. Can. J. Fish. Aquat. Sci. 106 (1), 110–127.

Koks, E.E., Rozenberg, J., Zorn, C., Tariverdi, M., Vousdoukas, M., Fraser, S.A., Hall, J. W., Hallegatte, S., 2019. A global multi-hazard risk analysis of road and railway infrastructure assets. Nat. Commun. 10 (1), 1–11.

Kulp, S.A., Strauss, B.H., 2019. New elevation data triple estimates of global vulnerability to sea-level rise and coastal flooding. Nat. Commun. 10 (1), 1–12.

Kummu, M., de Moel, H., Ward, P.J., Varis, O., Perc, M., 2011. How close do we live to water? A global analysis of population distance to freshwater bodies. PLoS ONE 6 (6), e20578.

Kummu, M., Ward, P.J., de Moel, H., Varis, O., 2010. Is physical water scarcity a new phenomenon? Global assessment of water shortage over the last two millennia. Environ. Res. Lett. 5 (3), 034006. https://doi.org/10.1088/1748-9326/5/3/034006.

Lawson, E., Thorne, C., Ahilan, S., Allen, D., Arthur, S., Everett, G., Fenner, R., Glenis, V., Guan, D., Hoang, L., Kilsby, C., 2014. Delivering and evaluating the multiple flood risk benefits in blue-green cities: An interdisciplinary approach. WIT Trans. Ecol. Environ. 184, 113–124.

Lehner, B., Döll, P., 2004. Development and validation of a global database of lakes, reservoirs and wetlands. J. Hydrol. 296 (1-4), 1–22.

Lloyd, C.T., Sorichetta, A., Tatem, A.J., 2017. High resolution global gridded data for use in population studies. Sci. Data 4 (1), 1–17.

Lugeri, N., Kundzewicz, Z.W., Genovese, E., Hochrainer, S., Radziejewski, M., 2010. River flood risk and adaptation in Europe-assessment of the present status. *Mitigation Adapt. Strateg. Global Change*. Mitig. Adapt. Strat. Glob. Change 15 (7), 621–639.

Mays, L.W., 2010. Water resources engineering. John Wiley & Sons, Hoboken, NJ.

Meijer, J.R., Huijbregts, M.A.J., Schotten, K.C.G.J., Schipper, A.M., 2018. Global patterns of current and future road infrastructure. Environ. Res. Lett. 13 (6), 064006. https://doi.org/10.1088/1748-9326/aabd42.

Merz, B., Kreibich, H., Schwarze, R., Thieken, A., 2010. Review article "Assessment of economic flood damage". Natural Hazards and Earth System Science 10 (8), 1697–1724.

Millennium Ecosystem Assessment, 2005. Ecosystems and Human Well-being: Wetlands and Water Synthesis. World Resources Institute, Washington, D.C.

Nakaegawa, T., 2012. Comparison of water-related land cover types in six 1-km global land cover datasets. J. Hydrometeorol. 13 (2), 649–664.

Ngoc Chau, V., Holland, J., Cassells, S., Tuohy, M., 2013. Using GIS to map impacts upon agriculture from extreme floods in Vietnam. Appl. Geogr. 41, 65–74.

Papa, F., Prigent, C., Aires, F., Jimenez, C., Rossow, W.B., Matthews, E., 2010. Interannual variability of surface water extent at the global scale, 1993–2004. Journal of Geophysical Research: Atmospheres 115 (D12).

Peduzzi, P., Dao, H., Herold, C., Mouton, F., 2009. Assessing global exposure and vulnerability towards natural hazards: The disaster risk index. Natural Hazards and Earth System Science 9 (4), 1149–1159.

Pesaresi, M., Florczyk, A., Schiavina, M., Melchiorri, M., Maffenini, L., 2019. GHS settlement grid, updated and refined REGIO model 2014 in application to GHS-BUILT R2018A and GHS-POP R2019A, multitemporal (1975-1990-2000-2015), R2019A. European Commission, Joint Research Centre (JRC). doi:10.2905/42E8BE89-54FF-464E-BE7B-BF9E64DA5218.

Pradhan, B., 2009. Flood susceptible mapping and risk area delineation using logistic regression, GIS and remote sensing. Journal of Spatial Hydrology 9 (2), 1–18.

Prigent, C., Papa, F., Aires, F., Rossow, W.B., Matthews, E., 2007. Global inundation dynamics inferred from multiple satellite observations, 1993–2000. Journal of Geophysical Research: Atmospheres 112 (D12).

Richter, B.D., Postel, S., Revenga, C., Scudder, T., Lehner, B., Churchill, A., Chow, M., 2010. Lost in development's shadow: The downstream human consequences of dams. Water Altern. 3 (2), 14–42.

Salmon, J.M., Friedl, M.A., Frolking, S., Wisser, D., Douglas, E.M., 2015. Global rain-fed, irrigated, and paddy croplands: A new high resolution map derived from remote sensing, crop inventories and climate data. Int. J. Appl. Earth Obs. Geoinf. 38, 321–334.

Smith, A., Bates, P.D., Wing, O., Sampson, C., Quinn, N., Neal, J., 2019. New estimates of flood exposure in developing countries using high-resolution population data. Nat. Commun. 10 (1), 1814.

Stevens, F.R., Gaughan, A.E., Linard, C., Tatem, A.J., Amaral, L.A.N., 2015. Disaggregating census data for population mapping using Random forests with remotely-sensed and ancillary data. PLoS ONE 10 (2), e0107042. https://doi.org/10.1371/journal.pone.0107042.

Subbiah, A., Kishore, K., Center, A.D.P., 2001. Long-range climate forecasts for agriculture and food security. Asian Disaster Preparedness Center, Bangkok, Thailand.

Sulla-Menashe, D., Friedl, M.A., 2018. User Guide to Collection 6 MODIS Land Cover (MCD12Q1 and MCD12C1) Product. Reston, VA, USA, USGS.

Tellman, B., Sullivan, J.A., Kuhn, C., Kettner, A.J., Doyle, C.S., Brakenridge, G.R., Erickson, T.A., Slayback, D.A., 2021. Satellite imaging reveals increased proportion of population exposed to floods. Nature 596 (7870), 80–86.

Tockner, K., Stanford, J.A., 2002. Riverine flood plains: present state and future trends. Environ. Conserv. 29 (3), 308–330. https://doi.org/10.1017/S037689290200022X.

United Nations, 2010. World Urbanization Prospects: The 2009 Revision. Population Division of the Department of Economic and Social Affairs of the United Nations: http://esa.un.org/unpd/wup/.

United Nations Development Programme (UNDP), 2004. Reducing disaster risk: A challenge for development. United Nations Development Programme, Bureau for Crisis Prevention and Recovery, New York, 146.

United Nations Statistics Division, 2020. Standard country or area codes for statistical use (M49). [Data table]. Retrieved from https://unstats.un.org/unsd/methodology/m49/.

van Alphen, S., 2020. Room for the River: Innovation, or Tradition? The Case of the Noordwaard, Adaptive Strategies for Water Heritage, p. 309.

Verhoeven, J.T., Setter, T.L., 2010. Agricultural use of wetlands: opportunities and limitations. Annals of botany 105 (1), 155–163. https://doi.org/10.1093/aob/mcp172.

Ward, P.J., Jongman, B., Weiland, F.S., Bouwman, A., van Beek, R., Bierkens, M.F.P., Ligtvoet, W., Winsemius, H.C., 2013. Assessing flood risk at the global scale: model setup, results, and sensitivity. Environ. Res. Lett. 8 (4), 044019. https://doi.org/10.1088/1748-9326/8/4/044019.

Wheater, H., Evans, E., 2009. Land use, water management and future flood risk. Land use Policy 26, S251–S264.

Winsemius, H.C., Aerts, J.C., van Beek, L.P., Bierkens, M.F., Bouwmna, A., Jongman, B., Kwadijk, J.C., Ligtvoet, W., Lucas, P.L., van Vuuren, D.P., Ward, P.J., 2016. Global drivers of future river flood risk. Nat. Clim. Change 6 (4), 381–385.

Winsemius, H.C., Van Beek, L.P.H., Jongman, B., Ward, P.J., Bouwman, A., 2013. A framework for global river flood risk assessments. Hydrol. Earth Syst. Sci. 17 (5), 1871–1892.

WorldPop (www.worldpop.org - School of Geography and Environmental Science, University of Southampton; Department of Geography and Geosciences, University of Louisville; Departement de Geographie, Universite de Namur) and Center for International Earth Science Information Network (CIESIN), Columbia University, 2018. Global High Resolution Population Denominators Project - Funded by The Bill and Melinda Gates Foundation (OPP1134076). https://dx.doi.org/10.5258/SOTON/WP00645.

Zhang, Q., Gu, X., Singh, V.P., Kong, D., Chen, X., 2015. Spatiotemporal behavior of floods and droughts and their impacts on agriculture in China. Global Planet. Change 131, 63–72.

Zhong, Q., Wang, K., Lai, Q., Zhang, C., Zheng, L., Wang, J., 2015. Carbon dioxide fluxes and their environmental control in a reclaimed coastal wetland in the Yangtze estuary. Estuaries Coasts 1–19.